Bank re-erosion action to promote sediment supply and channel diversification: Feedback from a restoration test on the Rhine

Valentin Chardon, Laurent Schmitt, Anne Clutier

River Research and Applications

Bank re-erosion action to promote sediment supply and channel diversification: Feedback from a restoration test on the Rhine

Journal:	*River Research and Applications*
Manuscript ID	RRA-22-0004
Wiley - Manuscript type:	Research Article
Date Submitted by the Author:	07-Jan-2022
Complete List of Authors:	CHARDON, Valentin; CNRS UMR 7362 LIVE University of Strasbourg Strasbourg France Schmitt, Laurent; CNRS UMR 7362 LIVE University of Strasbourg Strasbourg France Clutier, Anne; EDF Centre d'Ingenierie Hydraulique
Keywords:	Large river restoration, bank re-erosion, transverse groynes, geomorphological monitoring, management guidelines, Rhine river

Bank re-erosion action to promote sediment supply and channel diversification: Feedback from a restoration test on the Rhine

Valentin Chardon[1], Laurent Schmitt [1] & Anne Clutier [2]
Corresponding author: valentin.chardon@live-cnrs.unistra.fr
[1] CNRS UMR 7362 LIVE, University of Strasbourg, Strasbourg, France
[2] Electricité de France (EDF), Centre d'Ingénieurie Hydraulique (CIH), Le Bourget-du-Lac, France

Abstract

River regulation alters hydrological and sediment regimes and consequently affects habitat complexity and dynamics, biodiversity and ecosystem services. Although channel bank erosion is a key geomorphological process supplying alluvial channels with coarse sediments and diversifying aquatic and riparian habitats, banks have often been stabilized to limit erosion risk to human activities and facilities. The objective of this paper is to assess the effects, and their sustainability, of bank protection removal on a 300 m long reach of the Old Rhine (France/Germany) to promote sediment supply, channel diversification and a rehabilitation of fluvial morpho-sedimentary processes. This action was combined with the construction of two transverse groynes to locally increase bank erosion processes. Yearly detailed monitoring was implemented over 6 years, including classical bathymetric surveys, airborne topo-bathymetric and terrestrial LiDAR, and bed grain-size and bedload tracking. Following a Q_{15} flood, the restoration induced a weak sediment supply. The restoration diversified habitats due to the implementation of the two transverse groynes, inducing bank scouring and the creation of new macroforms, as well as local bed grain-size diversification and fining. The cross-sectional diversity of the restored water channel was close to the regularization engineering phase. Channel bedform diversification persisted six years due to the persistence of the two transverse groynes. The action induced the rehabilitation of fluvial forms, in a static manner, rather than the rehabilitation of fluvial morpho-sedimentary processes, which raises questions about the sustainability of the benefits of such management actions in terms of fluvial functionality and naturality.

Keywords: Large river restoration, bank re-erosion, transverse groynes, geomorphological monitoring, management guidelines, Rhine river

1. Introduction

Most rivers have been regulated for navigation, agriculture, flood protection and electricity production purposes, altering both hydrological and sediment regimes. River regulation affects geomorphological conditions and dynamics (bed incision, bed armouring, channel narrowing, etc.), as well as the complexity of aquatic and riverine habitats and associated biodiversity and ecosystem services (Kondolf, 1997).

During the last three decades, the number of river restorations has significantly increased around the world, notably in Europe, as encouraged by the Water Framework Directive (WFD), which targets the "good status of water bodies" (Morandi et al. 2017; Buisson et al. 2018). Restoration-linked monitoring (before-after and/or control impacted schemes are generally used) is crucial to evaluate restoration success by comparing the obtained results with the restoration objectives based on indicators. This feedback allows formulation of management recommendations focusing on the surveyed reach for further improvements and/or transferring restoration guidelines to similar river reaches (Shahverdian et al. 2019).

Several restoration strategies are commonly deployed to counteract sediment starvation conditions and channel simplification in regulated rivers. These strategies include gravel

augmentation (Arnaud et al. 2017; Kondolf et al. 2004; Gaeuman 2014; Chardon et al. 2021), bank re-erosion (Klösch et al. 2013) , remobilization of old vegetated sediment deposits (Landon, 2008; Thorel et al. 2018), dam removal (Foley et al. 2017; Poulos et al. 2019) and specific engineering actions aiming to reduce sediment trapping in dam reservoirs (Sumi, 2006). These actions may be combined to enhance geomorphological processes in a more sustainable way, e.g., on the Mür River (Klösch et al. 2013). Gravel augmentation consists of injecting a significant sediment volume downstream of dams according to the transport capacity of the river reach to limit sediment starvation and to restore fish habitats(Kondolf ,1997). Bank re-erosion actions may complexify and dynamize both riparian and aquatic habitats and may foster biodiversity (Hooke 1979; Florsheim, Mount, and Chin 2008; Habersack and Piégay 2007; Requena, Weichert, and Minor 2006). Whereas gravel augmentation has been well accepted by managers for several decades, bank erosion has until recently been regarded negatively because it may affect human activities and facilities (Hooke 1979; Florsheim, Mount, and Chin 2008), whereas the benefits of the rehabilitation of the "freedom river space" have been widely demonstrated (Piégay et al. 2005; Biron et al. 2014; Ciotti et al. 2021; Choné and Biron 2016). Recently, several river restorations based on controlled bank re-erosion of formerly stabilized banks, based on various technical protocols, were performed in Europe (Habersack and Piégay 2007). For example, on the Meuse River, riprap removal to diversify aquatic habitats was tested (Duró et al. 2020). On the Danube River, both removing bank protection and reshaping groynes were tested to complexify habitats and create refuges for native juvenile fish species (Ramler and Keckeis 2019). Nevertheless, the feedback of such restoration actions remains scarce at the world scale (Staentzel et al. 2020).

The aim of this study is to assess the capacity of a controlled bank re-erosion test carried out on the Old Rhine (France/Germany) to diversify both aquatic and riverine habitats linked to sediment supply from bank re-erosion. This test consisted of removing 300 m of historical bank protections on the left riverbank. The implementation of two transverse groynes was to maximize bank re-erosion.

We hypothesized that the action (i) would promote a high sediment supply to the channel from bank erosion, (ii) would diversify aquatic habitats and (iii) would allow the recovery of fluvial morpho-sedimentary processes such as coarse sediment erosion, transport and deposition (which may induce the formation of in-channel bars and side channels). To test these three hypotheses while evaluating the success of the action, hydrogeomorphological monitoring was conducted over six years. It combined (i) topo-bathymetric surveys, (ii) grain-size surveys and (iii) bedload tracking. Historical topo-bathymetric data were also used to compare post-restoration dynamics with the Old Rhine historical trajectory.

Figure 1. a. The Rhine Basin; b. locations of the Old Rhine, Grand Canal d'Alsace (GCA), dams, power plants and restoration site; c. removal of bank protection; d. groyne construction; and e. channel responses after the flood of May-June 2013 (left bank re-erosion and sediment deposition downstream of the upstream groyne; the view is in the downstream direction).

2. Materials and methods

2.1. Study area

The Rhine River is the third largest river in Europe, with a length and drainage area of 1,250 km and 185,000 km^2, respectively. The upper Rhine is located in a 300 km long tectonic graben between Basel and Bingen-am-Rhein and is characterized by a nivoglacial

hydrological regime. The mean annual discharge is estimated at 1,059 $m^3.s^{-1}$ in Basel (time period: 1891-2008) (Uehlinger et al. 2009). Since the beginning of the 19th century, the upper Rhine was profoundly impacted by three successive engineering works: (i) channelization (19th century), (ii) regularization, which consisted of the construction of alternate groyne fields (beginning and middle of the 20th century) and (iii) damming, and in some cases, flow diversion (middle of the 20th century up to 1977) (Fig. 1b). These works induced severe degradation of both geomorphological and ecological functionality, notably along the Old Rhine, which is a 50 km reach between Basel and Breisach that is bypassed by the Grand Canal d'Alsace (GCA) (Arnaud et al. 2015; Arnaud et al. 2019) . The instream flow varied between 20 and 30 m^3/s before December 2010. Since this date, it has varied between 52 $m^3.s^{-1}$ (winter) and 150 $m^3.s^{-1}$ (spring-summer) according to flow requirements for aquatic and riparian biocenoses in the frame of the Kembs Dam relicensing (Garnier and Barillier 2015) (Fig. 1b). Spill floods into the Old Rhine occur when the discharge in the GCA exceeds 1400 $m^3.s^{-1}$ at the Basel gauging station. An ambitious restoration programme was achieved between 2010 and 2017 to enhance the bedload and habitat dynamics by performing three gravel augmentations (2010, 2015, and 2016) and three controlled-bank re-erosions (one in 2013 and two in 2017) (Chardon et al. 2021; Aelbrecht et al. 2014)).

During April and May 2013, a first test of controlled bank re-erosion was performed (Fig. 1b-c). It consisted of removing historical (almost 2 centuries old) bank protection over a length of 300 m and removing three old groynes (almost 1 century old; Fig. 1). Additionally, two new transverse groynes were implemented to maximize bank re-erosion (Fig. 1d). The best locations and shapes of these groynes to favour bank re-erosion were determined prior to field work from numerical and physical modelling (Die Moran, 2012).

These studies showed that the groynes should be placed perpendicular to the bank and disconnected from it, with a length equal to 30 m.

Geomorphological monitoring was undertaken according to the before-after framework based on five states (Si) and four periods (Pi) (Fig. 2). The instantaneous peak flow estimated at the Rheinweiler gauging station (Fig. 1.b) was 3,070 $m^3.s^{-1}$ (Q_{ix}= 15 years), 1,910 $m^3.s^{-1}$ ($Q_{ix} \approx 5$ years), 1,880 $m^3.s^{-1}$ (Qix ≈ 5 years), and 2,010 $m^3.s^{-1}$ ($Q_{ix} \approx 5$ years) during P1, P2, P3, and P4, respectively.

Figure 2. Monitoring framework and maximum daily discharges recorded at the Rheinweiler gauging station in the Old Rhine.

2.2. Estimated sediment supply from bank re-erosion

2.2.1. Channel morphodynamic adjustments and sediment budgeting

Classical bathymetric surveys and airborne topo-bathymetric LiDAR surveys were performed to quantify the channel morphological adjustments. During S0, a Tritech PA500 single beam echo sounder was used to survey the topography of the wetted channel on a 1 km length reach. Since S1, yearly airborne topo-bathymetric LiDAR surveys have been performed to characterize the above-water and underwater channel topography along the first 20 km of the Old Rhine. This method combined two wavelengths: near-infrared (1,064 nm), which allows collecting datasets above the water level, and green (532 nm), which penetrates into the water column (Mandlburger et al. 2015; Chardon et al. 2019) . This technique provides high-resolution data, with averages of 20-40 pts/m^2 and 10 pts/m^2 in above-water and underwater conditions, respectively. The Riegl VQ-820-G sensor was used at S1, and the Optech Titan sensor was used at S2. For each state, high-resolution digital elevation models (DEMs) with a cell size of 0.25 m^2 were produced to assess both channel morphological adjustments and diachronic sediment budgets by the DEM of difference (DoD). ArcMap v.10.3 software was used to perform DEM production by applying the IDW interpolation method and to calculate the diachronic sediment budgets.

Terrestrial LiDAR surveys were also performed along the bank to estimate bank re-erosion. These surveys were achieved using a Leica HDS6200 sensor and a set of targets to georeference the point clouds. Target positions were recorded by real-time differential GNSS measurements made possible with the Teria network for planimetry and the NGF benchmarks for altimetry using a Spectra SP80 system.

We estimated the uncertainty of topo-bathymetric evolution for each Pi using the combined elevation change errors between two diachronic DEMs, according to the equation developed by (Brasington, Langham, and Rumsby, 2003) :

$$\sigma_{diff} = \sqrt{(\sigma_t)^2 + (\sigma_{(t+1)})^2} \quad (1)$$

where σ_t and σ_{t+1} are the estimated registration errors for each DEM (m). The registration errors were estimated to be equal to 0.10 m and 0.05 m for topo-bathymetric surveys and terrestrial LiDAR surveys, respectively.

A t test statistic, according to (Bennett et al. 2012) , was calculated to identify only elevation changes that were statistically significant when |t|>1 and t was calculated as follows:

$$t = \frac{(Z_{(t+1)} - Z_t)}{\sigma_{diff}} \quad (2)$$

where Z_t and Z_{t+1} are the elevations at t and t_{+1}, respectively.

We estimated the calculation errors of the volumes for each period P_i according to the following equation developed by (Lane, Westaway, and Hicks, 2003) :

$$\sigma_v = d^2\sqrt{n}\sigma_{(diff)} \quad (3)$$

where d is the cell size of the DEM (m) and n is the sum of the number of cells of deposited and eroded areas.

2.2.2. Bedload tracking

We equipped 1,050 bedload particles with passive transponders (PIT tags) with a 23 mm length developed by Texas Instruments to assess the travel distance of sediment coming from the eroded bank. The tracer grain-size classes ranged from 22.6 mm to 181 mm, and the D_{50} was equal to 58 mm. The tracer grain-size distribution was close to the natural surface grain-size distribution of a natural lateral bar located upstream of the study site. Tracers were located before the first flood of May-June 2013 (S0) along seven transects on the bank, each composed of three injection points of 50 tracers (bank toe, intermediate location and top of the bank) (Fig. 2). The initial positions of all tracers were obtained using a global positioning system (Trimble GeoXT 600, centimetric precision).

Bedload-tracking surveys were achieved using a CIPAM mobile loop antenna (diameter = 0.46 m) on the restored bank and in the channel where the water depth was below 0.8 m. Tracer positions were recorded using the GPS for punctual data recording. For water depths exceeding 0.8 m, a rectangular loop (width = 1.20 m) was pulled with a boat using cords of known length. A reader system developed by CIPAM was used to collect the unique identifier code of each recovered tracer. Tracer positions were determined using the GPS in continuous recording mode (time step recording equal to 1 s) and corrected by adding the cord length. The georeferenced errors of bedload tracers were estimated as 2 m and 5 m for the tracking performed by foot and by boat, respectively.

To link sediment mobility with flood energy, we calculated the excess peak stream power ($w.m^{-2}$) for each period Pi using the following equation (Petit, Perpinien, and Deroanne, 2000) :

$$W_{(pi)} = \frac{p_w g(Q_{pi} - Q_c) * S}{W} \quad (4)$$

where ρ_w is the water density ($kg.m^{-3}$), g is the acceleration due to gravity ($m.s^{-2}$), Q_{pi} is the instantaneous peak discharge for each period ($m^3.s^{-1}$), Q_c is the critical discharge ($m^3.s^{-1}$), S is the average local bed slope ($m.m^{-1}$) (calculated over a distance of 1000 m) and W is the bankfull mean active channel width (m). When several flood events occurred during one period, we summed the excess peak stream power of all peak floods that occurred

during the study period. The value of the critical discharge was estimated from a one-dimensional hydrosedimentary model and was equal to 550 $m^3.s^{-1}$ (El Kadi Abderrezzak 2009).

2.3. Indicator of channel diversity

2.3.1. Bedforms

For each Si, we calculated the channel topographic diversity of the water channel using the cross-section diversity (CSD) index developed by (Gostner et al. 2013) to quantify the channel morphological changes over time before and after the action and calculated it as follows:

$$CSD = \frac{\sum_{i=2}^{n} |\Delta Z_i|}{\sum_{i=1}^{n-1} X_i} \quad (5)$$

with

$$|\Delta Z_i| = Z_{(i-1)} - Z_i$$

where $|\Delta Z_i|$ is the absolute height difference between two consecutive points along the cross-section (m) and X_i is the distance between them (m).

We also calculated this index based on historical topo-bathymetric data (since 1884) that were produced along the 44 km length of the reach of the Rhine. This was performed to compare the channel post-restoration response with the Old Rhine morphology and processes of the corrected Rhine before regularization and canalization (Table 1). For 1884, the water levels were extracted from historical plans, while for the other periods, the water levels were extracted from aerial photographs (Table 1).

2.3.2. Grain size

For S0, the grain-size survey was focused on two emerged gravel bars located 200-500 m upstream and downstream of the controlled bank erosion site following the 100-particle protocol of (Wolman, 1954) (n=6). For S1, ten particles were sampled every 5 to 10 m in both underwater and above-water conditions along 65 cross-sections spaced at 10 m intervals, corresponding to the restored bank plus 350 m downstream. The length of the transects was approximately 40 to 50 m from the restored bank. When the water level exceeded 0.8 m, the survey was performed by diving. Since S2, when the water level exceeded 0.8 m, the survey was performed by both diving and telescopic bars from a boat using a GoPro Hero 4+ or an Olympus TG-4. When the water depth was below 0.8 m, Wolman manual sampling (10 particles) was used as during S1. To minimize underestimation of grain size by photoseiving compared with manual sampling related to particle imbrication or burial (Graham et al. 2010) , we aleatorically sampled ten particles that were completely visible on each image using a grid. This step was performed using the grid tool implemented with ImageJ v.1.51j8 software. The pixel size was determined using a rule placed at the bottom of a telescopic bar and with knowledge of the acquisition height during diving.

3. Results

3.1. Sediment supply

3.1.1. Bank re-erosion monitoring

Most bank re-erosion occurred during P1 following the Q_{15} flood of May-June 2013 (S1). The maximal bank retreat was equal to 4.31 m and was located close to the upstream groyne, with the creation of an erosion notch (Table 2; Fig. 1e). The total bank re-erosion volume reached 1,456 m^3, with 62% of this total volume coming from the notch. During P2, the erosion volume decreased significantly by one order of magnitude and was equal to

191 m^3. During P3, bank re-erosion occurred only on the notch, with an eroded volume equal to 26 m^3 (Table 2), while no bank re-erosion occurred during P4.
Important channel morphological changes occurred during P1, with the formation of two mid-bars downstream of the groynes, as well as the scouring of two pools (9,366 m^3) in the centre of the channel close to the groyne eastern extremities (Fig. 3a). A volume of 5,798 m^3 of sediments was deposited in the channel along the restored bank, including both mid-bars. This sediment volume corresponded to approximately 4 times that provided by bank re-erosion (Table 2) but was approximately half the total erosion volume (10,822 m^3), corresponding to bank re-erosion plus the scouring of the pools. During P2, the channel adjustments were weaker than those during P1, with an erosion tendency on the two mid-bars (-535 m^3 and -332 m^3 for the upstream mid-bar and downstream mid-bars, respectively) and the downstream pool (-420 m^3) and sediment deposition on the upstream pool (368 m^3) (Table 2; Fig. 3b). During P3, global erosion dynamics occurred in all geomorphic units (Table 2; Fig. 3c). The dynamics were globally inversed during P_4, with global weak dynamics of sediment deposition in all geomorphic units (Table 2; Fig. 3d). A tendency of slumping and erosion of both groynes was observed during the whole monitoring period (Table 2), with erosion volumes of -83 m^3 and -102 m^3 for the upstream and downstream groynes, respectively.

Figure 3. Channel changes during the monitoring: a. between S0 and S1 (P1), b. between S1 and S2 (P2), c. between S2 and S3 (P3), d. between S3 and S4 (P4) and e. between S0 and S4 (whole monitoring period). Grey polygons correspond to the groynes. Black points correspond to recovered bedload tracers. The dashed line in a represents the top of the restored bank, while UG and DG correspond to the upstream and downstream groynes, respectively.

3.1.2. Bedload monitoring

The recovery rates for S1, S2 and S3 were 8%, 22%, and 12%, respectively. Low recovery rates were due to the collision phenomenon between tracers located on the bank (42). The percentages of the same mobile tracers between two successive states were 58%, 10%, and 13% for periods P1, P2, and P3, respectively. The mean tracer travel distances for mobile tracers were 25 m, 14 m, and 269 m for periods P1, P2, and P3, respectively (Fig. 4a). The maximal distances were 205 m, 32 m, and 2,316 m for P1, P2, and P3, respectively. The recovered bedload tracers were mostly deposited at the two mid-channel bars located downstream of the two groynes (Fig. 3a-c). A comparison of tracer mobility between surveys shows an inverse law between the mean travel distance and excess peak stream energy (Fig. 4.b). Moreover, for an equivalent excess peak stream power, the mean travel distances were lower during P1 and P2 on the restored bank than for the three gravel augmentations performed in the Old Rhine mentioned above (Fig. 4b, 39). During P3, the relative mean travel distances of the tracers of the study reach were close to the empirical law based on the survey of the three gravel augmentations.

Figure 4. The results of bedload-tracking surveys: a. travel distances of mobile tracers for each period and b. mean travel distance of mobile tracers according to the excess peak stream power for the study reach. The data for three gravel augmentations performed on the Old Rhine are also shown for comparison purposes (data from Arnaud et al. 2017; Chardon et al. 2021). The empirical linear relationship corresponds to all surveys of the gravel augmentations.

3.2. Channel diversity

3.2.1. Bedforms

From historical topo-bathymetric data collected along the entire Old Rhine, the results

show a significant decrease in the values of the CSD index from 1884 to 1950/56, during which regularization engineering works were carried out (Fig. 5). A statistically significant, but relatively low, increase in the CSD index occurred between 1985/93 and 2009 (Fig. 5) due to high bed changes induced by the Q_{100} flood in 1999 and the Q_{50} flood in 2007 (Arnaud et al. 2019). At the restoration spatial scale, a significant increase in the CSD values occurred between S0 and S1 (Fig. 5). After S1, the CSD values continued to increase slightly between S2 and S4 (Fig. 5). The mean CSD value calculated for S0 at the restored site was close to the mean value for the whole Old Rhine after regularization, while the mean CSD values calculated from S1 to S4 corresponded to those before regularization (O. R 1884) (Table 3).

Figure. 5 Diachronic evolution of the cross-sectional diversity (CSD) index. White and grey boxplots correspond to the CSD index values calculated along the restored bank and the whole Old Rhine, respectively. Indicated values below boxplots correspond to the P values of the post hoc pairwise Mann–Whitney test. Paired and nonpaired Mann–Whitney U testing was performed at the different states for the restored bank and the entire Old Rhine reach, respectively. O.R corresponds to the entire Old Rhine. n corresponds to the number of cross-sections.

3.2.2. Grain size

The bed grain-size monitoring showed that the restoration induced grain-size refinement and diversification in comparison with the pre-restoration data (Fig. 6). The grain-size refinement reached 29 mm (D_{50}; -59%) for the gravel bars in above-water conditions (EMB) during P3 and 38 mm (D_{50}; -46%) during P1 for the gravel bars in underwater conditions (UMB). Grain-size diversification also occurred, with an increase of +44% in the Inman-sorting index during P2 for the EMB and +20% during P3 for the UMB. Grain-size changes in both the EMB and UMB were sustainable during the entire monitoring period (Fig. 6). On the other hand, grain-size fining and diversification on the remaining monitored reach (RMR) during P1 and P2 were transitory. During S3, the grain-size conditions of this part of the reach were comparable to the pre-restoration conditions (S0; Fig. 6)

Figure 6. Temporal grain-size evolution of the whole study reach (ALL; A.), the mid-channel bars in underwater conditions (UMB; B.), the mid-channel bars in emerged conditions (EMB; C.), the remaining monitored reach (RMR; D.) and evolution of the Inman-sorting index for each condition (E.). Percentages at each state were calculated by comparing the corresponding grain size with the grain size at S0. The sorting index was calculated following the equation proposed by (Inman, 1952) .

4. Discussion

4.1. Unexpected weak bank erosion

Our results show that major bank retreat occurred during P1 after the Q_{15} flood (1,456 m^3 eroded volume). During this flood, the main sediment supply provided from the local erosion notch was close to the upstream groyne (Table 2). This eroded volume represented ~8% of the annual sediment deficit of the Old Rhine, which was estimated at 16,000 m^3/y (Arnaud, 2012) . Through comparison with flume experiments, the modelled bank erosion volume was equal to 7,094 m^3 for a modelled Q_{10} flood (Die Moran et al. 2013) . These results show that field bank re-erosion was approximately half of one order of magnitude lower than expected. Since P2, bank erosion has been quasi-negligible due to several factors that may have limited bank erosion: (i) the concentration on the bank foot surface of historical riprap blocks, which were previously buried into the bank and whose size exceeds the river competence (the whole length of 300 m is considered; Fig.

1.e); (ii) local outcrops of Pleistocene coarse pudding sediment located in the bank foot (Fig. 1.e); (iii) excessively weak local hydraulic conditions despite the presence of groynes; and (iv) the progressive vegetation growth of the bank that began since P2. These results show that the management action provided no significant bank re-erosion, which invalidates our first hypothesis.

To increase the success of this kind of action, it would be best to perform a sounding (depth of 2-4 m) to check if riprap blocks are buried within the bank and to remove them if necessary to avoid bank foot pavement and stabilization. This approach seems particularly important for banks that have been stabilized for a long period (more than a century), which may have been reworked several times to ensure stabilization in the past. In addition, bank erosion processes may be enhanced using logjams (Krzeminska et al. 2019; Sukhodolov, Uijttewaal, and Engelhardt, 2002) and increasing bank irregularity to increase hydraulic condition complexity or to implement artificial macroforms (Gaeuman, 2014).

4.2. Groynes increased channel diversification and effect duration of the management action

The restoration action induced clear bedform diversification along a channel length of 650 m, with the formation of two gravel bars and two pools (located at the eastern extremity of the groynes), as well as surface grain-size diversification and fining (Fig. 2.; Fig. 6). The bed topographic changes occurred after high flows (mainly the first flood) driven by the implementation of the two groynes. They induced, downstream of them, a local decrease in flow conditions and the presence of countercurrents (Sukhodolov, Uijttewaal, and Engelhardt 2002; Yossef, 2002) , which induced the formation of the two gravel deposits (Fig. 3). The groynes also induced the scouring of two pools at the centre of the channel (Fig. 3). This was explained by a local increase in shear stresses due to the channel tightening induced by the two groynes. The sediment volume deposited on the two mid-bars (5,798 m^3; P1) was much higher than the sediment volume provided by bank re-erosion (1,456 m^3; P1). This shows that deposited sediment was also supplied from the scouring of the two pools (9,366 m^3; P1) (Fig. 3; Table 2) and probably also from residual morphodynamics of the Old Rhine upstream of the restored bank(Arnaud et al. 2015) . The bed grain-size diversification and fining that occurred along the whole restored length and downstream along a total length of 600 m (Fig. 6) was induced by the abovementioned sediment supply and the reduced hydraulic conditions and countercurrents downstream of the groynes. Moreover, the action also significantly diversified the overall riverbed morphology. While the CSD index values exhibited a strong negative morphological impact of the regularization works (first half of the 20th century), the restoration induced a significant unexpected recovery of the morphological diversity comparable to that before the regularization (Fig. 5; Table 3). This mainly resulted in the implementation of the two transverse groynes. Interestingly, the CSD index values revealed a relatively weak but significant morphological diversification from 1985/93 to 2009 (Fig. 5) due to two high flood events during this period (Q_{100} in 1999 and Q_{50} in 2007; (Arnaud et al. 2015). Post-restoration geomorphological evolution induced positive ecological effects in the short term, such as an increase in the diversity and richness of macroinvertebrate, fish and macrophyte communities (Aelbrecht et al. 2014; Staentzel et al. 2018; 2019) . An ecological habitat-modelling approach also highlighted a significant increase in habitat suitability for several lentic fish species (Chardon et al. 2020) .

Both topo-bathymetric and RFID monitoring results show that the sustainability of the effects of the restoration action depended mainly on the persistence of the two groynes. The local erosion areas of the two mid-bars from P2 to P4 were the consequence of a partial slump of the two groynes, especially the upstream one, which was most impacted by high water velocities during floods (Table 2). The field monitoring showed that bedload

velocity along the restored bank increased over time despite a temporal decrease in the excess peak energy due to the progressive partial slump of the groynes. For comparable values of excess peak energy, bedload velocities during P1 and P2 were much lower than the bedload transit below three gravel augmentations implemented in the Old Rhine some kilometres upstream of the study site, which was the consequence of the low hydraulic conditions on the two mid-bars induced by the two groynes (Fig. 4; Yossef, 2002). However, once the tracers left the two mid-bars (P3), the transfer velocities were comparable to those calculated for the three gravel augmentations (Fig. 4.a). These results highlight that to promote sustainable habitat diversification on regulated rivers, sediment deposition and habitat diversification depend notably on the presence of areas of low water velocities that could be created by channel topo-bathymetric diversity. All of these results show that the second hypothesis was partially validated. Indeed, the action promoted bed diversification, but this diversification was mainly linked to the implementation of transverse groynes rather than the inputs of sediment from bank re-erosion.

4.3. Feedback for further management guidelines: focusing on processes rather than forms

Our results showed that the action promoted channel bedform diversity and bed grain-size diversification. However, these effects were not based on morpho-sedimentary processes, which invalidated our third hypothesis and raised some questions about the sustainability of the benefits of such management actions. A question remains whether habitat diversification is sufficient following groyne installation or if the targeted species also need bed morphodynamic changes in the mid/long term. To rehabilitate morpho-sedimentary processes on regulated rivers affected by sediment starvation conditions, such as the Old Rhine, it appears meaningful to implement bed widening some kilometres downstream of gravel augmentations (Arnaud et al. 2017; Klösch et al. 2013; Chardon et al. 2018). Indeed, this approach would foster sediment deposition, the creation of new fluvial forms and local bank re-erosion, thus diversifying habitats (bars, secondary channels, etc.) and recovering geomorphic processes, which may optimize the effects of restoration actions in terms of both efficiency and sustainability. Excavated sediment from artificial channel widening could be used for upstream gravel augmentation after a temporary storage period, with the duration depending on flood frequencies and intensities (Chardon et al. 2021).

5. Conclusion

This study provides an original evaluation of groyne implementation and bank protection removal on a 300 m long reach of the Old Rhine (France/Germany) to increase sediment supply and promote bedform diversification. Our results show that low sediment volumes were injected into the channel from bank re-erosion due to the (i) concentration on the bank foot surface of historical riprap blocks, (ii) local outcrops of Pleistocene coarse sediment on the bank foot, (iii) excessively weak local hydraulic conditions despite the presence of the groynes and (iv) progressive vegetation growth on the bank. Following the action, a high diversification of aquatic and riverine habitats occurred with the creation of new macroforms and the fining and diversification of the bed grain size, which was mainly attributed to the implementation of the two transverse groynes. However, these changes were attributed mainly to the implementation of the two transverse groynes rather than bank re-erosion. Moreover, the sustainability of the effects of the action depends on the persistence of the groynes. This action induced the rehabilitation of fluvial forms in a static manner rather than the rehabilitation of fluvial morpho-sedimentary processes, which raises questions about the sustainability of the benefits of such management actions. For large sediment-starved rivers, it appears meaningful to implement bed widening some

kilometres downstream of gravel augmentation (Arnaud et al. 2017; Chardon et al. 2018), which would foster sediment deposition, the creation of new fluvial forms and local bank erosion. This management could diversify both aquatic and riparian habitats and restore geomorphic processes, thus increasing the efficiency and sustainability of such actions (Chardon et al. 2021).

Bibliography

Aelbrecht, D, A Clutier, A Barillier, K Pinte, K El-Kadi-Abderrezzak, A Die-Moran, F Lebert, and A Garnier. 2014. 'Morphodynamics Restoration of the Old Rhine through Controlled Bank Erosion: Concept, Laboratory Modeling, and Field Testing and First Results on a Pilot Site'. *River Flow 2014*, no. August: 2397–2403. https://doi.org/10.1201/b17133-319.

Arnaud, F., H. Piégay, L. Schmitt, A.J. Rollet, V. Ferrier, and D. Béal. 2015. 'Historical Geomorphic Analysis (1932–2011) of a by-Passed River Reach in Process-Based Restoration Perspectives: The Old Rhine Downstream of the Kembs Diversion Dam (France, Germany)'. *Geomorphology* 236 (May): 163–77. https://doi.org/10.1016/j.geomorph.2015.02.009.

Arnaud, Fanny. 2012. 'Approches Géomorphologiques Historique et Expérimentale Pour La Restauration de La Dynamique Sédimentaire d' Un Tronçon Fluvial Aménagé : Le Cas Du Vieux Rhin Entre Kembs et Breisach (France, Allemagne)', 1–280.

Arnaud, Fanny, Hervé Piégay, David Béal, Pierre Collery, Lise Vaudor, and Anne-Julia Rollet. 2017. 'Monitoring Gravel Augmentation in a Large Regulated River and Implications for Process-Based Restoration: MONITORING GRAVEL AUGMENTATION IN A LARGE REGULATED RIVER'. *Earth Surface Processes and Landforms* 42 (13): 2147–66. https://doi.org/10.1002/esp.4161.

Arnaud, Fanny, Laurent Schmitt, Karen Johnstone, Anne-Julia Rollet, and Hervé Piégay. 2019. 'Engineering Impacts on the Upper Rhine Channel and Floodplain over Two Centuries'. *Geomorphology* 330 (April): 13–27. https://doi.org/10.1016/j.geomorph.2019.01.004.

Bennett, Georgina Lucy, P. Molnar, H. Eisenbeiss, and Brian W Mcardell. 2012. 'Erosional Power in the Swiss Alps: Characterization of Slope Failure in the Illgraben'. *Earth Surface Processes and Landforms* 37 (15): 1627–40. https://doi.org/10.1002/esp.3263.

Biron, Pascale M., Thomas Buffin-Bélanger, Marie Larocque, Guénolé Choné, Claude-André Cloutier, Marie-Audray Ouellet, Sylvio Demers, Taylor Olsen, Claude Desjarlais, and Joanna Eyquem. 2014. 'Freedom Space for Rivers: A Sustainable Management Approach to Enhance River Resilience'. *Environmental Management* 54 (5): 1056–73. https://doi.org/10.1007/s00267-014-0366-z.

Brasington, James, Joe Langham, and Barbara Rumsby. 2003. 'Methodological Sensitivity of Morphometric Estimates of Coarse Fluvial Sediment Transport'. *Geomorphology* 53 (3–4): 299–316. https://doi.org/10.1016/S0169-555X(02)00320-3.

Buisson, Elise, Renaud Jaunatre, Baptiste Regnery, Marthe Lucas, Jean-François Alignan, Alma Heckenroth, Isabelle Muller, et al. 2018. 'Promoting Ecological Restoration in France: Issues and Solutions: Restoration in France'. *Restoration Ecology* 26 (1): 36–44. https://doi.org/10.1111/rec.12648.

Chardon, Valentin, Laurent Schmitt, Fanny Arnaud, Hervé Piégay, and Anne Clutier. 2021. 'Efficiency and Sustainability of Gravel Augmentation to Restore Large Regulated Rivers: Insights from Three Experiments on the Rhine River (France/Germany)'. *Geomorphology* 380 (May): 107639. https://doi.org/10.1016/j.geomorph.2021.107639.

Chardon, Valentin, Laurent Schmitt, Hervé Piégay, Fanny Arnaud, Jordane Serouilou, Jérôme Houssier, and Anne Clutier. 2018. 'Geomorphic Effects of Gravel Augmentation on the Old Rhine River Downstream from the Kembs Dam (France, Germany)'. *E3S Web of Conferences* 40: 02028. https://doi.org/10.1051/e3sconf/20184002028.

Chardon, Valentin, Laurent Schmitt, Hervé Piégay, Jean-Nicolas Beisel, Cybill Staentzel, Agnès Barillier, and Anne Clutier. 2020. 'Effects of Transverse Groynes on Meso-Habitat

Suitability for Native Fish Species on a Regulated By-Passed Large River: A Case Study along the Rhine River'. *Water* 12 (4): 987. https://doi.org/10.3390/w12040987.

Chardon, Valentin, Laurent Schmitt, Hervé Piégay, and Dimitri Lague. 2019. 'Use of Terrestrial Photosieving and Airborne Topographic LiDAR to Assess Bed Grain Size in Large Rivers: Potentials and Limits Journal': *Earth Surface Processes and Landforms*. https://ejournal3.undip.ac.id/index.php/jamt/article/view/5101.

Choné, G., and P. M. Biron. 2016. 'Assessing the Relationship Between River Mobility and Habitat: RELATIONSHIP BETWEEN MOBILITY AND HABITAT'. *River Research and Applications* 32 (4): 528–39. https://doi.org/10.1002/rra.2896.

Ciotti, Damion C, Jared Mckee, Karen L Pope, G Mathias Kondolf, and Michael M Pollock. 2021. 'Design Criteria for Process-Based Restoration of Fluvial Systems'. *BioScience* 71 (8): 831–45. https://doi.org/10.1093/biosci/biab065.

Die Moran, Andrés. 2012. 'Physical and Numerical Modelling Investigation of Induced Bank Erosion as a Sediment Transport Restoration Strategy for Trained Rivers. The Case of the Old Rhine (France)', 243.

Die Moran, Andrés, Kamal El Kadi Abderrezzak, Erik Mosselman, Helmut Habersack, Franck Lebert, Denis Aelbrecht, and Eric Laperrousaz. 2013. 'Physical Model Experiments for Sediment Supply to the Old Rhine through Induced Bank Erosion'. *International Journal of Sediment Research* 28 (4): 431–47. https://doi.org/10.1016/S1001-6279(14)60003-2.

Douglas L. Inman. 1952. 'Measures for Describing the Size Distribution of Sediments'. *SEPM Journal of Sedimentary Research* Vol. 22 (3): 125–45. https://doi.org/10.1306/D42694DB-2B26-11D7-8648000102C1865D.

Duró, Gonzalo, Alessandra Crosato, Maarten G. Kleinhans, Timotheus G. Winkels, Hessel A.G. Woolderink, and Wim S.J. Uijttewaal. 2020. 'Distinct Patterns of Bank Erosion in a Navigable Regulated River'. *Earth Surface Processes and Landforms* 45 (2): 361–74. https://doi.org/10.1002/esp.4736.

El Kadi Abderrezzak, Kamal. 2009. 'Report H-P73-2009-00402-FR', 1–26.

Florsheim, Joan L., Jeffrey F. Mount, and Anne Chin. 2008. 'Bank Erosion as a Desirable Attribute of Rivers'. *BioScience* 58 (6): 519. https://doi.org/10.1641/B580608.

Foley, Melissa M, Francis J Magilligan, Christian E Torgersen, Jon J Major, Chauncey W Anderson, Patrick J Connolly, Daniel Wieferich, et al. 2017. 'Dam Removal-Listening in Landscape Context and the Biophysical Response of Rivers to Dam Removal in the United States', no. January 2018. https://doi.org/10.1371/journal.pone.0180107.

Gaeuman, D. 2014. 'HIGH-FLOW GRAVEL INJECTION FOR CONSTRUCTING DESIGNED IN-CHANNEL FEATURES' 706 (May 2013): 685–706. https://doi.org/10.1002/rra.

Garnier, Alain, and Agnès Barillier. 2015. 'The Kembs Project: Environmental Integration of a Large Existing Hydropower Scheme'. *La Houille Blanche*, no. 4 (August): 21–28. https://doi.org/10.1051/lhb/20150041.

Gostner, Walter, Maria Alp, Anton J. Schleiss, and Christopher T. Robinson. 2013. 'The Hydro-Morphological Index of Diversity: A Tool for Describing Habitat Heterogeneity in River Engineering Projects'. *Hydrobiologia* 712 (1): 43–60. https://doi.org/10.1007/s10750-012-1288-5.

Graham, David J., Anne-Julia Rollet, Hervé Piégay, and Stephen P. Rice. 2010. 'Maximizing the Accuracy of Image-Based Surface Sediment Sampling Techniques: IMAGE-BASED SURFACE SEDIMENT SAMPLING'. *Water Resources Research* 46 (2). https://doi.org/10.1029/2008WR006940.

Habersack, Helmut, and Hervé Piégay. 2007. '27 River Restoration in the Alps and Their Surroundings: Past Experience and Future Challenges'. In *Developments in Earth Surface Processes*, 11:703–35. Elsevier. https://doi.org/10.1016/S0928-2025(07)11161-5.

Hooke, J.M. 1979. 'An Analysis of the Processes of River Bank Erosion'. *Journal of Hydrology* 42 (1–2): 39–62. https://doi.org/10.1016/0022-1694(79)90005-2.

Klösch, M., R. Hornich, N. Baumann, G. Puchner, and H. Habersack. 2013. 'Mitigating Channel

Incision Via Sediment Input and Self-Initiated Riverbank Erosion at the Mur River, Austria'. In *Geophysical Monograph Series*, edited by Andrew Simon, Sean J. Bennett, and Janine M. Castro, 319–36. Washington, D. C.: American Geophysical Union. https://doi.org/10.1029/2010GM000977.

Kondolf, G. Mathias. 1997. 'PROFILE: Hungry Water: Effects of Dams and Gravel Mining on River Channels'. *Environmental Management* 21 (4): 533–51. https://doi.org/10.1007/s002679900048.

Kondolf, G Mathias, J Toby Minear, G Mathias Kondolf, Ward Street, and Berkeley Ca. 2004. 'Coarse Sediment Augmentation on the Trinity River Below Lewiston Dam : Geomorphic Perspectives and Review of Past Projects Report to the Trinity River Restoration Program Introduction and Scope Append Ix A', no. September.

Krzeminska, Dominika, Tjibbe Kerkhof, Kamilla Skaalsveen, and Jannes Stolte. 2019. 'Effect of Riparian Vegetation on Stream Bank Stability in Small Agricultural Catchments'. *CATENA* 172 (January): 87–96. https://doi.org/10.1016/j.catena.2018.08.014.

Landon, Norbert. 2008. 'Du Constat d ' Enfoncement Du Lit Fluvial Aux Actions de Recharge Sédimentaire : Quelles Solutions Pour Une Gestion Raisonnée de Nos Cours d ' Eau ? To Cite This Version : HAL Id : Halshs-00279895 Outils de Gestion de l ' Eau En Territoire de Montagne'.

Lane, Stuart N., Richard M. Westaway, and D Murray Hicks. 2003. 'Estimation of Erosion and Deposition Volumes in a Large, Gravel-Bed, Braided River Using Synoptic Remote Sensing'. *Earth Surface Processes and Landforms* 28 (3): 249–71. https://doi.org/10.1002/esp.483.

Mandlburger, Gottfried, Christoph Hauer, Martin Wieser, and Norbert Pfeifer. 2015. 'Topo-Bathymetric LiDAR for Monitoring River Morphodynamics and Instream Habitats-A Case Study at the Pielach River'. *Remote Sensing* 7 (5): 6160–95. https://doi.org/10.3390/rs70506160.

Morandi, Bertrand, Jochem Kail, Anne Toedter, Christian Wolter, and Hervé Piégay. 2017. 'Diverse Approaches to Implement and Monitor River Restoration: A Comparative Perspective in France and Germany'. *Environmental Management* 60 (5): 931–46. https://doi.org/10.1007/s00267-017-0923-3.

Petit, François, Geoffrey Perpinien, and Carl Deroanne. 2000. 'Détermination des puissances spécifiques critiques dans des rivières à charge de fond caillouteuse'. *Revue Géographique de l'Est* 40 (1–2). https://doi.org/10.4000/rge.4203.

Piégay, Hervé, S. E. Darby, E. Mosselman, and N. Surian. 2005. 'A Review of Techniques Available for Delimiting the Erodible River Corridor: A Sustainable Approach to Managing Bank Erosion'. *River Research and Applications* 21 (7): 773–89. https://doi.org/10.1002/rra.881.

Poulos, Helen M., Kate E. Miller, Ross Heinemann, Michelle L. Kraczkowski, Adam W. Whelchel, and Barry Chernoff. 2019. 'Dam Removal Effects on Benthic Macroinvertebrate Dynamics: A New England Stream Case Study (Connecticut, USA)'. *Sustainability* 11 (10): 2875. https://doi.org/10.3390/su11102875.

Ramler, David, and Hubert Keckeis. 2019. 'Effects of Large-River Restoration Measures on Ecological Fish Guilds and Focal Species of Conservation in a Large European River (Danube, Austria)'. *Science of The Total Environment* 686 (October): 1076–89. https://doi.org/10.1016/j.scitotenv.2019.05.373.

Requena, P, R B Weichert, and H E Minor. 2006. 'Self Widening by Lateral Erosion in Gravel Bed Rivers'. *River Flow 2006, Vols 1 and 2*, 1801–9.

Shahverdian, Scott. n.d. 'CHAPTER 3: PLANNING FOR LOW-TECH PROCESS-BASED RESTORATION', 58.

Staentzel, Cybill, Jean-Nicolas Beisel, Sébastien Gallet, Laurent Hardion, Agnès Barillier, and Isabelle Combroux. 2018. 'A Multiscale Assessment Protocol to Quantify Effects of Restoration Works on Alluvial Vegetation Communities'. *Ecological Indicators* 90 (July):

643–52. https://doi.org/10.1016/j.ecolind.2018.03.050.
Staentzel, Cybill, Isabelle Combroux, Agnès Barillier, Corinne Grac, Etienne Chanez, and Jean-Nicolas Beisel. 2019. 'Effects of a River Restoration Project along the Old Rhine River (France-Germany): Response of Macroinvertebrate Communities'. *Ecological Engineering* 127 (February): 114–24. https://doi.org/10.1016/j.ecoleng.2018.10.024.
Staentzel, Cybill, G. Mathias Kondolf, Laurent Schmitt, Isabelle Combroux, Agnès Barillier, and Jean-Nicolas Beisel. 2020. 'Restoring Fluvial Forms and Processes by Gravel Augmentation or Bank Erosion below Dams: A Systematic Review of Ecological Responses'. *Science of The Total Environment* 706 (March): 135743. https://doi.org/10.1016/j.scitotenv.2019.135743.
Sukhodolov, Alexander, Wim S.J. Uijttewaal, and Christof Engelhardt. 2002. 'On the Correspondence between Morphological and Hydrodynamical Patterns of Groyne Fields'. *Earth Surface Processes and Landforms* 27 (3): 289–305. https://doi.org/10.1002/esp.319.
Sumi, Tetsuya. n.d. 'DESIGNING AND OPERATING OF FLOOD RETENTION "DRY" DAMS IN JAPAN AND USA', 11.
Thorel, Maxine, Herve Piégay, Carole Barthelemy, Bianca Räpple, Charles Robin Gruel, Pierre Marmonier, Thierry Winiarski, et al. 2018. 'Socio-Environmental Implications of Process-Based Restoration Strategies in Large Rivers: Should We Remove Novel Ecosystems along the Rhône (France)?' *Regional Environmental Change*. https://doi.org/10.1007/s10113-018-1325-7.
Uehlinger, Urs, Hartmut Arndt, Karl M. Wantzen, and Rob S.E.W. Leuven. 2009. 'The Rhine River Basin'. In *Rivers of Europe*, 199–245. Elsevier. https://doi.org/10.1016/B978-0-12-369449-2.00006-0.
Wolman, M Gordon. 1954. 'A Method of Sampling Coarse River-Bed Material'.
Yossef, Mohamed F M. 2002. 'Literature Review The Effect of Groynes on Rivers'. *Delft University of Technology Faculty of Civil Engineering and Geosciences Section of Hydraulic Engineering*, no. January 2002: 58.

Acknowledgements

This research was supported by the company Electricité de France (EDF) within the research collaborations "Geomorphic monitoring of gravel augmentation experiment into the Old Rhine – years 2013-2014" (EDF 5500-4300937910) and "Redynamization of the Old Rhine – years 2014-2018" (EDF 5910132058). The authors thank colleagues who provided fieldwork assistance: J. Houssier, J. Serouilou, G. Skupinski, D. Eschbach and F. Bruckmann. The authors also acknowledge the assistance provided by the Regierungspräsidium Freiburg (RPF), which provided a historical topographic dataset and SINTEGRA for the terrestrial LiDAR data. The authors also thank the laboratory Environnement Ville et Société (EVS UMR-5600), which performed the initial grain size survey.

Author contributions statement

V.C. and L.S. conceived of the experiments, V.C. and L.S. conducted the experiments, and V.C., L.S.,and A.C. analysed the results. All authors reviewed the manuscript.

Data availability statement

Data available on request from the authors.

Topographic dataset				Planimetric dataset – Water level extraction		
Year	Dataset source	Sector (KP)	Characteristics	Year	Source	Mean daily discharge ($m^3.s^{-1}$)
1884	Departmental archive (Plan)	174.00-218.00	16 cross-sections spaced to 3 km (30 to 40pts/cross-section)	1884	Plan	334.00–1640.00
1950/56	RPF(GIS)	174.40–214.00	Cross-sections spaced to 200 m (70 pts/cross-section)	1956	Aerial photography	37.00–39.00
1985/93	RPF(GIS)	174.40–209.93	Cross-sections spaced to 200 m (150 pts/cross-section)	1991-92	Aerial photography	35.00–54.00
2009	RPF(GIS)	174.10–220.80	Cross-sections spaced to 200 m (150 pts/cross-section)	2008	Aerial photography	39.00
2017	GeofitConseil (GIS)	174.00–209.00	Cross-sections spaced to 200 m (150 pts/cross-section)	2017	Aerial photography	78.00

Table 1. Characteristics of historical topo-bathymetric and planimetric datasets used to calculate the CSD index along the entire Old Rhine during a period of approximately 140 years. KP corresponds to kilometric points on the Rhine river. The mean daily discharges are provided from the Rheinweiler gauging station, except for 1884, for which discharges were provided from the Rheinhalle gauging station.

Geomorphic units	SB – P1 (m^3)	SB – P2 (m^3)	SB – P3 (m^3)	SB – P4 (m^3)
Whole bank	-1,456 ± (0.43)	191 ± (0.44)	-26 ± (0.43)	ns
Erosion notch	-890 ± (0.50)	-83 ± (0.59)	-26 ± (0.43)	ns
Upstream mid-bar	3,843 ± (5.42)	-535 ± (5.13)	-2,173 ± (5.26)	216 ± (3.28)
Downstream mid-bar	1,955 ± (7.32)	-332 ± (7.29)	-523 ± (5.25)	966 ± (6.45)
Upstream pool	-3,502 ± (3.10)	368± (3.13)	-1,884 ± (6.49)	368 ± (3.10)
Downstream pool	-5,864 ± (4.12)	-420 ± (4.16)	-2,254 ± (8.27)	1,466 ± (7.50)
Upstream groyne	-	-77 ± (1.28)	-	-6 ± (0.94)
Downstream groyne	-	-90 ± (1.46)	-	-12 ± (1.48)

Table 2. Diachronic sediment balances (SB) for each geomorphic unit of the study area. Geomorphic units are indicated in Fig. 3a. Values in brackets indicate the estimated errors, and ns indicates no significant changes.

State	O.R 1884	O.R 1950/56	O.R 1985/93	O.R 2009	O.R 2017
S_0	1.10^{e-05}	0.20	0.18	0.33	0.26
S_1	0.12	5.00^{e-09}	1.00^{e-08}	6.80^{e-06}	4.30^{e-07}
S_2	0.24	2.00^{e-10}	2.80^{e-10}	2.10^{e-07}	1.10^{e-09}
S_3	0.45	3.30^{e-12}	1.10^{e-12}	1.70^{e-09}	2.00^{e-12}
S_4	0.72	7.10^{e-11}	5.00^{e-11}	5.00^{e-08}	2.20^{e-10}

Table 3. P values resulting from the post hoc pairwise comparisons of the Mann–Whitney

1 U test between the CSD calculated along the restored bank and on the whole Old Rhine
2 (O.R).

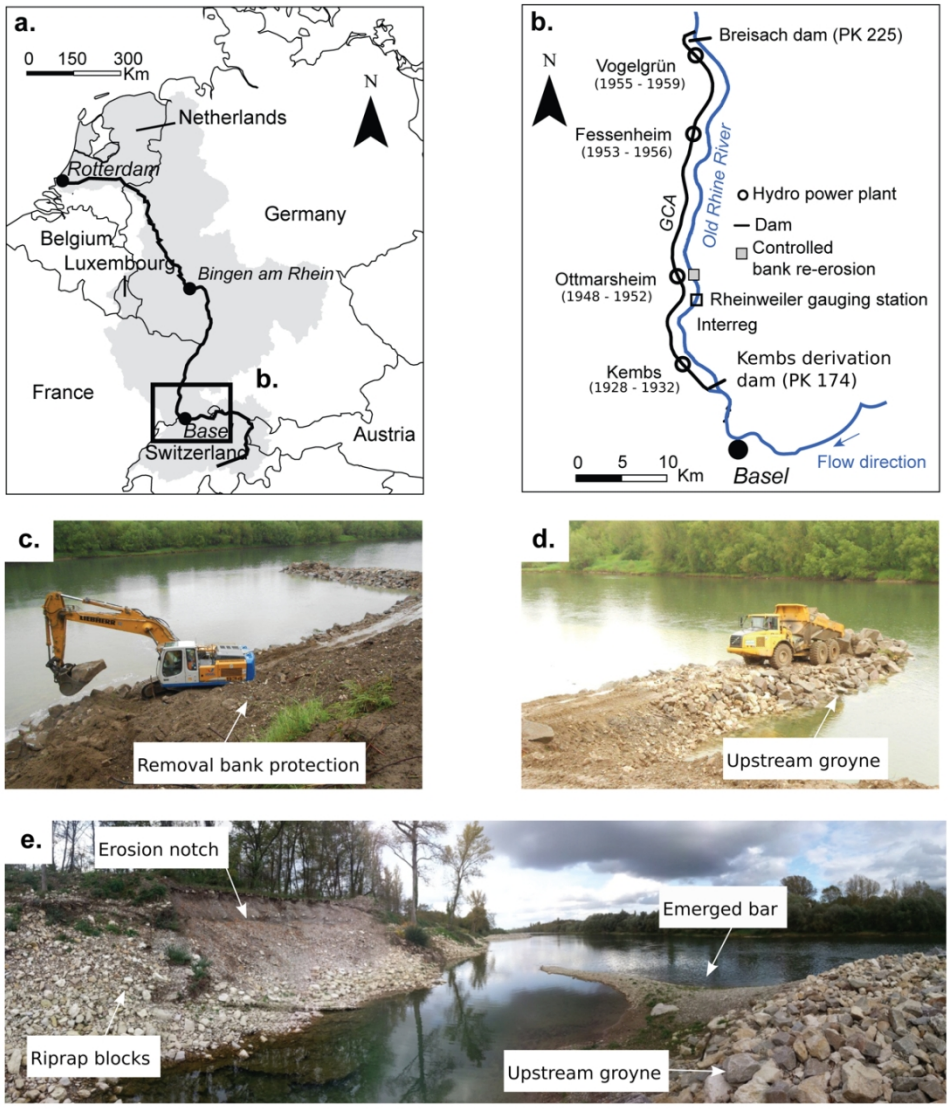

271x323mm (118 x 118 DPI)

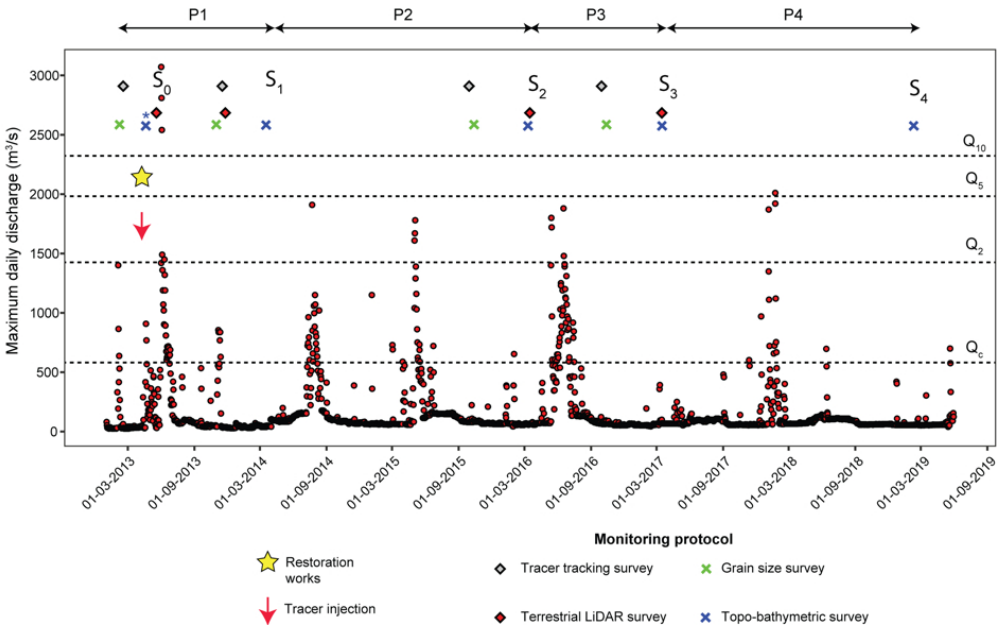

405x250mm (59 x 59 DPI)

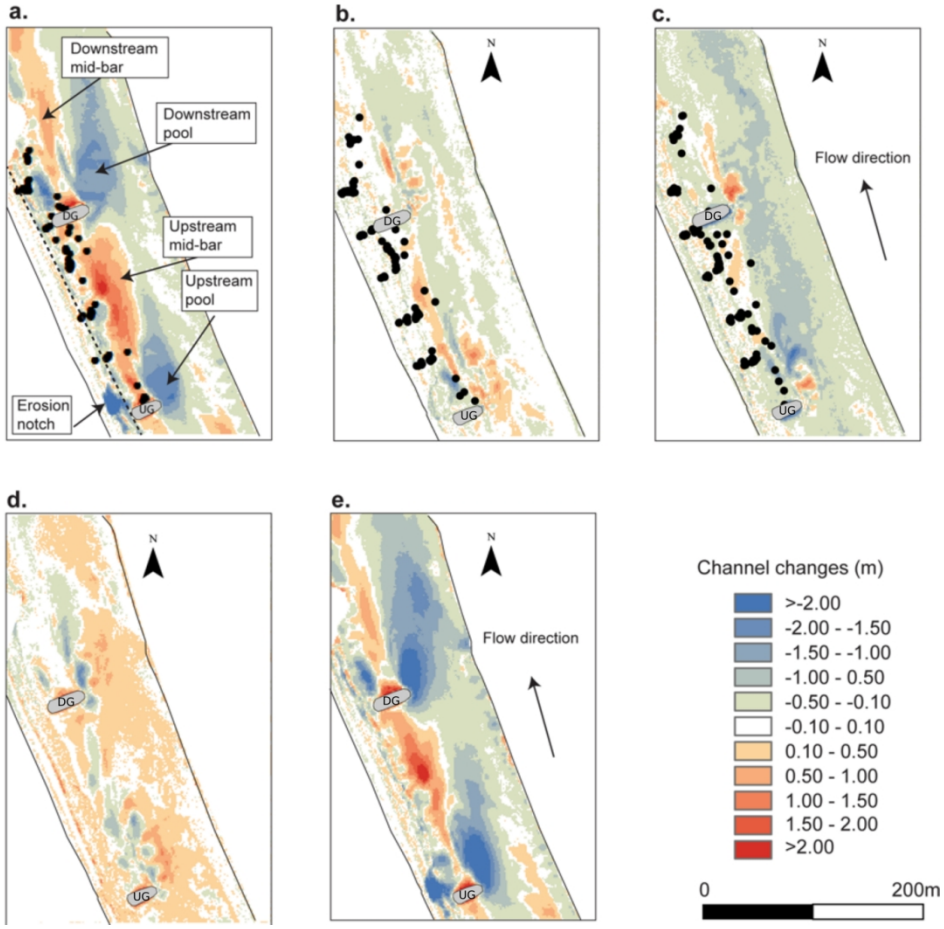

170x157mm (220 x 220 DPI)

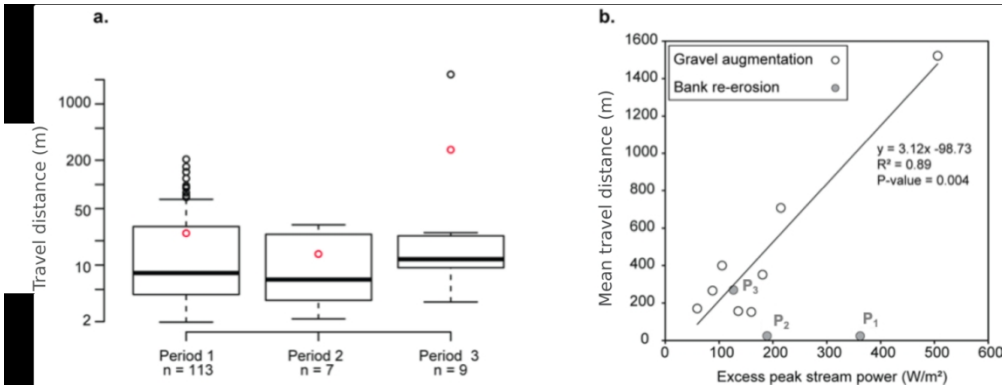

170x64mm (220 x 220 DPI)

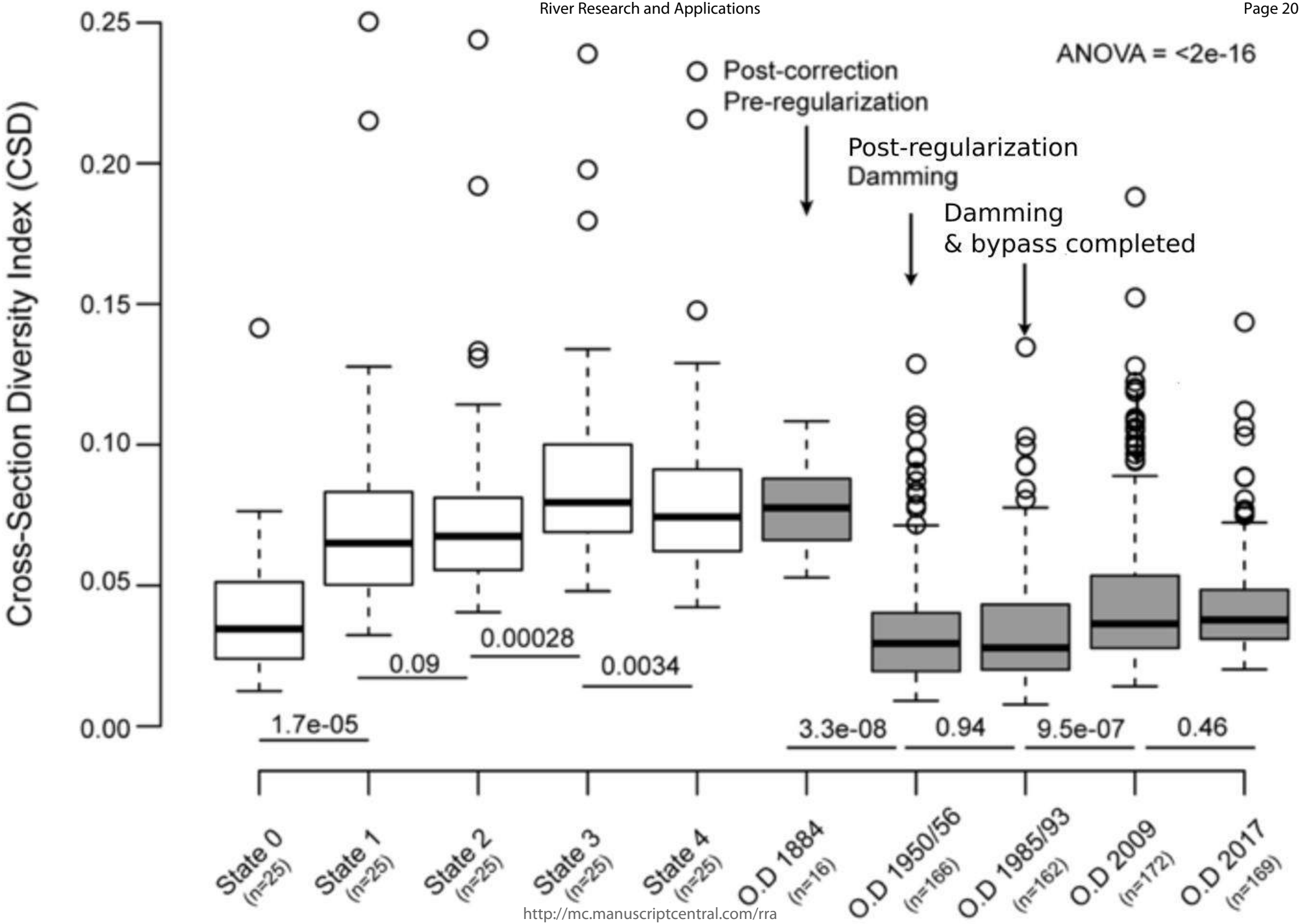
Cross-Section Diversity Index (CSD)
0.25
0.20
0.15
0.10
0.05
0.00
ANOVA = <2e-16
Post-correction
Pre-regularization
Post-regularization
Damming
Damming
& bypass completed
0.09
0.00028
0.0034
1.7e-05
3.3e-08
0.94
9.5e-07
0.46
State 0 (n=25)
State 1 (n=25)
State 2 (n=25)
State 3 (n=25)
State 4 (n=25)
O.D 1884 (n=16)
O.D 1950/56 (n=166)
O.D 1985/93 (n=162)
O.D 2009 (n=172)
O.D 2017 (n=169)

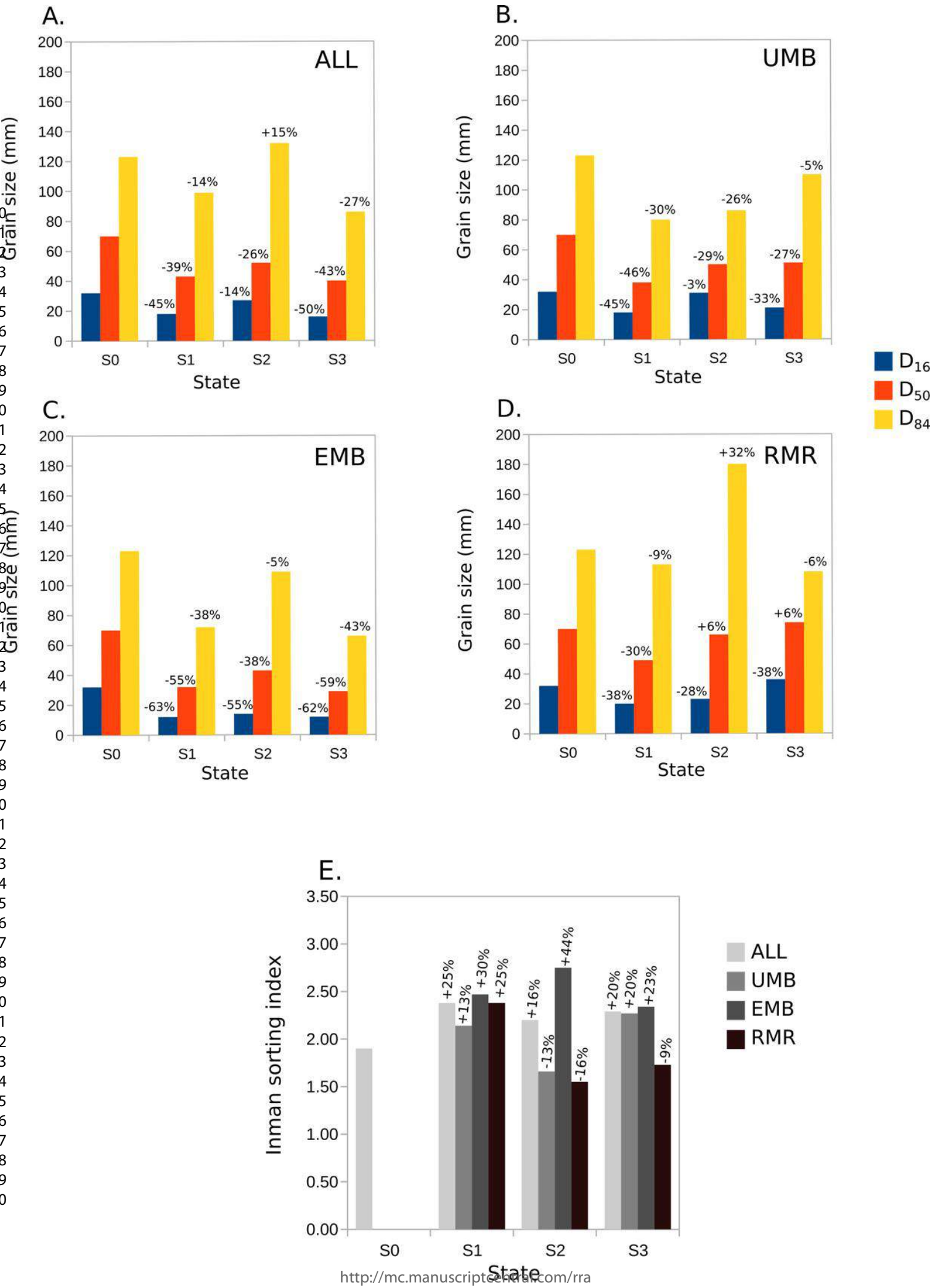
A.
ALL
B.
UMB
C.
EMB
D.
RMR
Grain size (mm)
State
S0
S1
S2
S3
D_{16}
D_{50}
D_{84}
E.
Inman sorting index
ALL
UMB
EMB
RMR